Use of physiologically based kinetic (PBK) modeling to study interindividual human variation and species differences in plasma concentrations of quercetin and its metabolites

Boonpawa, R., Moradi, N., Spenkelink, A., Rietjens, I. M. C. M., & Punt, A.

Use of physiologically based kinetic (PBK) modeling to study interindividual human variation and species differences in plasma concentrations of quercetin and its metabolites

Rungnapa Boonpawa[*a], Nooshin Moradi[a], Albertus Spenkelink[a], Ivonne M. C. M. Rietjens[a], and Ans Punt[a]

[a]Division of Toxicology, Wageningen University, Tuinlaan 5, 6703 HE Wageningen, The Netherlands.

*Corresponding author:

Rungnapa Boonpawa, Division of Toxicology, Wageningen University

Tuinlaan 5, 6703 HE Wageningen, The Netherlands.

Tel.: +31 317 482 294

Fax: +31 317 484 931

E-mail: Rungnapa2.Boonpawa@wur.nl; boonpawa_5@hotmail.com

Abbreviations

PBK, physiologically based kinetic; AUC, area under the curve; ADME, absorption, distribution, metabolism, excretion; Q4´Gly, quercetin-4´-O-glucoside; Q34´diGly, quercetin-3,4´-O-diglucoside; DMSO, dimethyl sulfoxide

Abstract

Biological activities of flavonoids *in vivo* ultimately depend on the systemic bioavailability of the aglycones and their metabolites. We aimed to develop physiologically based kinetic (PBK) models to predict plasma concentrations of the flavonoid quercetin and its metabolites in individual human subjects and to define species differences compared with male rat. The human models were developed based on *in vitro* metabolic parameters derived from incubations with pooled and 20 individual human tissue fractions and by fitting kinetic parameters to available *in vivo* data. The outcomes obtained were compared to a previously developed model for quercetin and its metabolites formation in male rat. Quercetin-3´-O-glucuronide was predicted to be the major circulating metabolite in 19 out of 20 individuals, while in male rat di- and tri-conjugates of quercetin containing a glucuronic acid, sulfate and/or methyl moiety are the major metabolites. Significant species differences occur in major circulating metabolites of quercetin suggesting that rat is not an adequate model to study effects of quercetin in man. The defined PBK models can be used to guide the experimental design of *in vitro* experiments with flavonoids, especially to better take into account the relevance of metabolism and the contribution of metabolites to the biological activity in humans.

Key words

quercetin; Absorption Distribution Metabolism Excretion (ADME); Physiologically Based Kinetic (PBK) modelling; species differences; human variation

1. Introduction

Flavonoids are polyphenolic compounds widely distributed in fruits and vegetables. These compounds have received a lot of attention for their possible beneficial health effects against various degenerative disorders such as cancer [1], cardiovascular diseases [2, 3], and obesity and diabetes [4]. A vast amount of *in vitro* studies have been conducted to elucidate modes of actions underlying these health effects. However, where most of these *in vitro* studies are performed with the aglycone, this form is hardly available *in vivo* due to extensive metabolism of the flavonoid aglycone in the intestine and liver. As a result, mainly flavonoid conjugates occur in the systemic circulation. Little is known about the nature and physiologically relevant concentrations of these circulating conjugates, nor about species differences and interindividual human variation herein. However, interpretation as well as design of both *in vitro* and *in vivo* animal and human experiments would benefit from insight in the nature and physiologically relevant concentrations of circulating conjugates. The aim of the present study was to use physiologically based kinetic (PBK) modeling to predict the nature and regiospecificity of the major circulating metabolites using quercetin as a model compound.

Quercetin is one of the most prevalent flavonoids in the human diet (e.g. onions) and also one of the most widely studied flavonoids [5]. Upon absorption, quercetin aglycone can be directly taken up in the small intestine by passive diffusion, but its glucoside needs to be deglycosylated to the aglycone by brush-border lactase phlorizin hydrolase or by intestinal microflora prior to absorption [6, 7]. In the small intestine and liver, quercetin is metabolized via glucuronidation, sulfation and methylation (Figure 1). Numerous mono-, di- and tri-conjugates of quercetin containing glucuronic acid, sulfate and/or methyl moieties have been detected in plasma of rat as well as in human [8-10]. Various metabolites have been reported as major circulating metabolites of quercetin in humans. Mullen *et al.* reported quercetin-3´-O-sulfate and quercetin-3-O-glucuronide to be among the major circulating metabolites 0.5 h after consumption of 270 g fried onions [10]. Lee *et al*. found that quercetin monoglucuronides are major circulating

metabolites 0.5 h after consumption of 47.5 g onion powder [9]. Another study by Day *et al.* reported that the major circulating metabolites of quercetin in plasma 1.5 h after consumption of 200 g fried onions, are quercetin-3-O-glucuronide, 3´-O-methylquercetin-3-O-glucuronide, and quercetin-3´-O-sulfate [11]. In comparison, in rats the major circulating metabolite detected 1 h after dosing of 7.6 mg/kg bw quercetin-4´-O-glucoside (Q4´Gly) was a tri-conjugate containing glucuronic acid, sulfate and methyl moieties [8]. Based on our previous PBK model studies, this tri-conjugate in rat was tentatively identified as 7-O-glucuronide,-3´-O-sulfate,-4´-O-methylquercetin [12].

To obtain better insights in the nature and concentration of circulating metabolites of quercetin and interindividual human variation, PBK models for quercetin in (individual) humans were defined based on kinetic parameters for the formation of different metabolites obtained from *in vitro* incubations with relevant individual and pooled human tissue fractions and by fitting kinetic parameters to the available *in vivo* data [9-11]. A subsequent comparison was made with the previous defined PBK model for quercetin in male rats [12] to elucidate possible species differences in the major circulating metabolites.

2. Material and methods

2.1 Materials

Pooled, mixed-gender human small intestine and liver S9 fractions, individual human liver S9 fractions from 20 different individual, and pooled human liver cytosol were purchased from Xenotech (Lenexa, USA). Quercetin, L-ascorbic acid, uridine 5′-diphosphoglucuronic acid (purity 98%), S-(5′-adenosyl)-L-methionine (purity 80%), 3′-phosphoadenosine 5′-phosphosulfate (purity 65%,), tris (hydroxymethyl)aminomethane, alamethicin (from *Trichoderma viride*), and β-glucuronidase/sulfatase (from *Helix pomatia*) were purchased from Sigma-Aldrich (Steinheim, Germany). Potassium dihydrogen phosphate, dipotassium hydrogen phosphate trihydrate, acetic acid (glacial), hydrochloric acid (fuming 37%), ammonium acetate, magnesium chloride, sodium acetate trihydrate, and trifluoroacetic acid (for spectroscopy) were purchased from VWR International (Darmstadt, Germany). Dimethyl sulfoxide (DMSO) was purchased from Acros Organic (New Jersey, USA). Acetonitrile (ULC/MS) and methanol (ULC/MS) were purchased from Biosolve (Valkenswaard, The Netherlands). Quercetin-3-O-glucuronide, isorhamnetin (3′-O-methylquercetin), and tamarixetin (4′-O-methylquercetin) were purchased from Extrasynthese (Genay Cedex, France).

2.2 Glucuronidation of quercetin by pooled and individual human tissue fractions

To obtain kinetic parameters for glucuronidation of quercetin, incubation mixtures (final volume of 100 µl) were prepared containing (final concentrations) 0.1 M Tris-HCl (pH 7.4), 10 mM $MgCl_2$, 1 mM ascorbic acid, 0.04 mg/ml pooled human small intestine or 0.03 mg/ml pooled liver S9 fractions, and 4 mM uridine 5′-diphosphoglucuronic acid as cofactor. The incubation mixtures were pre-treated on ice with 0.025 mg/ml alamethicin added from a 200 times concentrated stock solution in methanol for 15 min to obtain optimal glucuronidation activity [13]. The reactions were initiated by adding quercetin (final concentrations ranging from 0.15 µM to 20 µM) added from 200 times concentrated stock solutions in DMSO after preincubating at

37ºC for 1 min. The reactions were terminated by adding 25 µl ice-cold acetonitrile:acetic acid (94:6) (v/v) after 6 min or 7 min for incubations with small intestine S9 or liver S9. To evaluate interindividual human variation in glucuronidation, incubations with individual human liver S9 fractions were performed as described for pooled liver S9. These reactions were carried out for 5 to 20 min at 37ºC and at an S9 protein content ranging from 0.01 to 0.03 mg/ml, depending on the human subject. Under the specified conditions, the formation of quercetin monoglucuronides was linear in time and with protein concentration (data not shown). The nature of the glucuronide metabolites was confirmed by treating samples with β-glucuronidase (β-glucuronidase/sulfatase). For these reactions, 50 µl of the non-terminated mixtures were added to 50 µl of 0.1 M sodium acetate (pH 5.0) containing 1 mM ascorbic acid and 0.8 units/ml β-glucuronidase. These incubations were carried for 1 h at 37ºC and terminated by addition of 25 µl ice-cold acetonitrile:acetic acid (94:6) (v/v).

2.3 Sulfation of quercetin by pooled and individual human tissue fractions

To obtain kinetic parameters for sulfation of quercetin, incubation mixtures (final volume of 100 µl) were prepared containing (final concentrations) 0.1 M potassium phosphate (pH 7.4), 1 mM ascorbic acid, 0.2 mg/ml pooled human small intestine or 1 mg/ml pooled liver S9 fractions, and 0.1 mM 3′-phosphoadenosine 5′-phosphosulfate as cofactor. Samples were preincubated at 37ºC for 1 min prior to the addition of quercetin (final concentration ranging from 0.15 µM to 4 µM) added from 200 times concentrated stock solutions in DMSO to initiate the reactions. The reactions were terminated after 12 min by the addition of 25 µl ice-cold acetonitrile:acetic acid (94:6) (v/v). To evaluate interindividual human variation in sulfation, incubations with individual human liver S9 fractions were performed as described for pooled liver S9. These reactions were carried out at an S9 protein content ranging from 0.2 to 0.8 mg/ml for 6 to 40 min, depending on the human subject. Under the specified conditions, the formation of quercetin sulfate conjugates was linear in time and with protein concentration (data not shown). Formation of the quercetin

sulfate conjugates was confirmed by adding 50 µl of a non-terminated mixture to 50 µl of 0.2 M potassium phosphate (pH 6.2) containing 1 mM ascorbic acid and 100 units/ml sulfatase (β-glucuronidase/sulfatase). These samples were incubated for 1 h at 37ºC and the reactions were terminated by addition of 25 µl ice-cold acetonitrile:acetic acid (94:6) (v/v). To determine whether the microsomal protein in S9, which can serve as a potential source of sulfatase enzymes could influence the rate of formation of the different sulfate conjugates, incubations were performed with cytosol [14, 15]. These reactions revealed proportionally the same kinetic constants as with S9 indicating no influence of microsomes on the reaction (data not shown).

2.4 Methylation of quercetin by pooled and individual human tissue fractions

To obtain kinetic parameters for methylation of quercetin, incubation mixtures (final volume 100 µl) were prepared containing (final concentrations) 0.1 M potassium phosphate (pH 7.4), 1 mM ascorbic acid, 1 mg/ml pooled human small intestine or 1 mg/ml pooled liver S9 fractions, and 2 mM S-(5′-adenosyl)-L-methionine as cofactor. The reactions were initiated by the addition of quercetin (final concentrations ranging from 0.25 µM to 40 µM) added from a 200 times concentrated stock solution in DMSO after 1 min preincubation at 37ºC. Upon incubating for 22 min, 25 µl ice-cold acetonitrile:acetic acid (94:6) (v/v) were added to terminate the reactions. To evaluate interindividual human variation in quercetin methylation, incubations with individual human liver S9 fractions were performed as described for pooled liver S9. These reactions were carried out at an S9 protein content ranging from 0.3 to 1 mg/ml for 15 to 122 min at 37ºC, depending on the human subject. Under the specified conditions, methylation of quercetin was linear in time and with protein concentration (data not shown).

2.5 UPLC analysis

Kinetic constants were obtained from triplicate incubations for pooled tissue fractions and duplicate incubations for individual human liver fractions. Blank incubations were carried out

without the cofactor. The amount of glucuronide, sulfate and methyl conjugates formed, was analyzed on a UPLC-DAD system consisting of a Waters (Milford, MA) Acquity binary solvent manager, sample manager, and photodiode array detector, equipped with a Waters Acquity UPLC BEH RP 18 column (1.7 μm, 2.1 x 50 mm). Before analysis, all samples were centrifuged at 18,600 x *g* for 5 min at 5ºC to precipitate proteins and 10 μl of the supernatant was immediately analyzed. For glucuronide conjugates, a gradient of 2.5 mM ammonium acetate in nanopure water (eluent A) and acetonitrile (eluent B), was used with a flow rate of 0.6 ml/min with the following profile: 10-25% B (0-1.8 min); 25-90% B (1.8-2.5 min); 90% B (2.5-3.8 min); 90-10% B (3.8-4 min) and 10% B (4-5 min). For sulfate and methyl conjugates, a gradient of nanopure water containing 0.1% (v/v) trifluoroacetic acid (eluent A) and acetonitrile (eluent B) was used with a flow rate of 0.6 ml/min with the following profile: 20-25% B (0-1.8 min); 25-35% B (1.8-2.3 min); 35% B (2.3-2.8 min); 35-100% B (2.8-3 min); 100% B (3-4.1 min); 100-0% B (4.1-4.3 min); 0% B (4.3-5.5 min); 0-20% B (5.5-5.6 min) and 20% B (5.6-5.8 min).

The metabolites obtained from glucuronidation and sulfation were identified by comparing the UV-spectra and the elution order of each metabolite with those reported in the studies of Boersma *et al.* [16] and van der Woude *et al.* [17] as described previously for incubations with rat tissue fractions [12]. The metabolites obtained from incubations measuring methylation were identified by comparing the UV-spectra and the retention time with commercially available standards of 3´-O-methylquercetin and 4´-O-methylquercetin. All quercetin metabolites were quantified by integrating the peak areas at 370 nm and by using the calibration curves of quercetin-3-O-glucuronide (for glucuronide conjugates), quercetin (for sulfate conjugates), and 3′-O-methylquercetin and 4´-O-methylquercetin (for methyl conjugates).

2.6 LC-MS analysis

The nature of the formed metabolites from glucuronidation, sulfation and methylation of quercetin was identified using LC-MS on a Perkin Elmer 200 series HPLC system (Perkin Elmer,

Waltham, MA) coupled to an API 3000 system (Applied Biosystem, Foster city, CA). Aliquots of 10 µl were injected on an Agilent Zorbax Extend-C18 column, 2.1 x 50 mm, 3.5 Micron 80 Å with a Zorbax guard column (Basel, Switzerland). The same gradient compositions as described in Section 2.5 were used, except that eluent A was nanopure water containing 0.1% (v/v) acetic acid and a flow rate of 0.2 ml/min was used with the following profile: 20% B (0-1 min), 20-35% B (1-4 min), 35% B (4-6 min), 35-80% B (6-10 min), 80% B (10-15 min), 80-20% B (15-16 min), and 20% B (16-20 min). The mass spectrometric analysis was performed in the negative ion mode using a spray voltage of 4.5 kV and a capillary temperature of 180ºC. The nebulizer gas (air), curtain (nitrogen), declustering potential, focusing potential, and entrance potential were set to 10, 8, -51, -200, and -13.7, respectively. Analysis was carried out using product ion (MS^2) scanning from *m/z* 200-600.

2.7 Kinetic analysis

Kinetic parameters (i.e. apparent maximum velocity ($V_{max(app)}$) and apparent Michaelis-Menten constant ($K_{m(app)}$)) for glucuronidation, sulfation, and methylation of quercetin were determined by fitting the data to the standard Michaelis-Menten equation:

$$v = V_{max} \times [S]/(K_m+[S]) \quad (1)$$

where [S] represents the substrate concentration. The data were fitted to the Michaelis-Menten equation with GraphPad Prism, version 5.04 (GraphPad Software, San Diego, California, USA).

2.8 Definition of the PBK model for (individual) human subjects

The PBK models that describe the absorption, distribution, metabolism and excretion (ADME) of quercetin in (individual) humans were defined in a similar manner as used for developing the previously defined PBK model for quercetin in male rats [12]. The structure of the models is displayed in Figure 2. The kinetic data describing metabolic conversion of quercetin to its primary metabolites were obtained in the present study based on the *in vitro* experiments (see

section 3.1-3.3). Even though quercetin is one of the most studied flavonoids, there are only few studies identifying and quantifying the plasma profiles of quercetin in humans [9-11]. Therefore, we only used these studies for the development of the models. The parameters describing excretion via urine, bile and intestinal enterocyte efflux back to lumen were fitted to the available experimental human data [9-11]. These data are primary available for onion intake, containing mainly Q4´Gly and quercetin-3,4´-O-diglucoside (Q34´diGly) [9, 10] and are hydrolyzed to the aglycone by luminal lactase phlorizin hydrolase [18, 19]. Thus disappearance of the glucosides to the aglycone in the intestinal lumen was included and fitted to the experimental data, assuming each glucoside has its own deglycosylation rate with values ranging from 0.51 – 1 l/h and 0.01 – 0.1 l/h for Q4´Gly and Q34´diGly, respectively. The uptake rate constant of quercetin aglycone to the small intestine in humans was assumed to be similar to rats with a value of 5.32 h^{-1} [20]. For the PBK model describing the ADME in an average human, the kinetic constants obtained from incubations with pooled human tissue fractions were used. Whereas for the PBK models in individual human subjects, the kinetic constants obtained with the individual human liver fractions were used. No interindividual human variation in metabolism by the small intestine was taken into account in the individual human models as the plasma concentrations of quercetin metabolites is mainly influenced by the kinetic constants for formation of primary metabolites in liver (see section 3.4).

For description of further conjugation of the primary metabolites to di- and tri-conjugates, only further conjugation of different monoglucuronides was simulated since the glucuronide metabolites were estimated to account for ~96% of the dose (see section 3.4). Lower catalytic efficiencies for further glucuronidation, sulfation, and methylation of the monoglucuronides to di- and tri-conjugates were assumed in comparison to the catalytic efficiencies for formation of the respective mono-conjugates, due to both an increase in K_m and a decrease in V_{max} [12]. The correction factors for further conjugation were obtained by fitting the predicted plasma AUC or concentrations to the available experimental data [9-11]. Taking the regiospecificity of possible

conjugations into account, a total of 34 different mono-, di- and tri-conjugates could in theory be expected and were thus included in the model.

The physiological parameters were obtained from the literature [21] and the partition coefficients were calculated based on the methods described by DeJongh *et al.* [22]. The physiological parameters and partition coefficients, thus obtained and used in the models are summarised in Table 1 and 2. Mass balance equations were numerically integrated in Berkeley Madonna 8.3.18 (Macey and Oster, UC Berkeley, CA) using the Rosenbrock's algorithm for stiff system. Mass balance equations for quercetin and its metabolites in tissues and blood were similar to those previously described in the PBK model for quercetin in male rats [12]. Model performance was assessed by comparing the predicted excretions via urine, bile and intestinal enterocyte efflux back to lumen against available *in vivo* data [10, 23, 24]. With the obtained model, the systemic bioavailability of quercetin aglycone and the nature and regiospecificity of the major circulating quercetin metabolites in plasma were predicted. Conversion of the blood concentrations of the different metabolites to plasma concentrations was done by dividing the blood concentrations by a blood/plasma ratio (R). For quercetin and its metabolites a R value of 0.66 was applied and calculated using Simcyp prediction tools [25, 26]. The systemic bioavailability of quercetin aglycone and the sensitivity analysis for the plasma $AUC_{0\text{-}24h}$ of quercetin metabolites were determined follow the methods previously described by Boonpawa *et al.* [12].

3. Results

3.1 Glucuronidation of quercetin by pooled and individual human tissue samples

Analysis of the incubations with pooled human liver and intestine S9 revealed that both fractions were able to metabolize quercetin towards different types of glucuronide conjugates. In incubations with human small intestine S9, quercetin-7-O-glucuronide, quercetin-3-O-glucuronide, quercetin-3′-O-glucuronide, and quercetin-4′-O-glucuronide were formed. The same metabolites, except for quercetin-4′-O-glucuronide, were formed in incubations with human liver S9. The LC-MS results confirmed that the formed metabolites were quercetin monoglucuronide as all formed metabolites had an M^- at *m/z* 477, which fragmented to produce *m/z* 301 (quercetin). The quercetin concentration dependent rate of formation of the monoglucuronides in these incubations with pooled liver or small intestine S9 is shown in Figure 3A and 3B. For both tissues, quercetin-3′-O-glucuronide was formed with the highest catalytic efficiency, which was 5 to 18-fold higher than the catalytic efficiency for formation of the other glucuronide conjugates in these tissues (Table 3).

Analysis of interindividual human variation in formation of monoglucuronides revealed 39-fold variation in the catalytic efficiencies for formation of these metabolites between the 20 individual human liver S9 samples that were analyzed (Table 4). Quercetin-7-O-glucuronide and quercetin-3′-O-glucuronide were formed with the highest catalytic efficiency by individual H0420 (male, Caucasian, 42 years) and quercetin-3-O-glucuronide by individual H0270 (male, Caucasian, 5 months). All three conjugates were formed with the lowest catalytic efficiency by individual H0291 (female, Caucasian, 18 years). The latter differences were due to both a ± 3-fold lower V_{max} and a ± 20-fold higher K_m for glucuronidation by individual H0291. The incubations with individual human liver S9 fractions also revealed that quercetin-3′-O-glucuronide is the predominant glucuronide formed by 18 out of 20 individual human liver S9.

3.2 Sulfation of quercetin by pooled and individual human tissue samples

Analysis of the incubations with pooled human liver and intestine S9 revealed that both fractions were able to metabolize quercetin to sulfate conjugates. Quercetin-3′-O-sulfate was the predominant sulfate metabolite formed in incubations with human intestine S9 and quercetin-7-O-sulfate was a minor metabolite. In incubations with human liver S9 only quercetin-3′-O-sulfate was formed. The LC-MS results confirmed that the formed metabolites were quercetin sulfate as all formed metabolites had an M^- at *m/z* 381, which fragmented to produce *m/z* 301 (quercetin). The quercetin concentration dependent rate of formation of the sulfate conjugates in these incubations with pooled human liver or small intestine S9 is shown in Figure 3C and 3D and the kinetic constants derived from these curves are displayed in Table 3.

In incubations with individual human liver S9 also only quercetin-3′-O-sulfate was formed, showing a 833-fold variation in formation of this metabolite between the different human samples (Table 5). The highest catalytic efficiency was observed for individual H0251 (female, Caucasian, 42 years), and the lowest for individual H0420 (male, Caucasian, 42 years). The differences between these individuals were due to 13- and 76-fold variation in the V_{max} and the K_m for sulfation respectively (Table 5).

3.3 Methylation of quercetin by pooled and individual human tissue samples

Analysis of the incubations with pooled human liver and intestine S9 revealed that only liver S9 was able to metabolize quercetin to methyl conjugates. In incubations with liver S9, both 3′-O-methylquercetin and 4′-O-methylquercetin were formed. The LC-MS results confirmed that the formed metabolites were quercetin methyl conjugates as all formed metabolites had an M^- at *m/z* 315, which fragmented to produce *m/z* 301 (quercetin). Figure 3E shows the quercetin concentration dependent rate of formation of methyl conjugates of quercetin in incubations with human liver S9 fractions and the kinetic constants derived from these curves are displayed in Table 3. The highest catalytic efficiency was observed in individual H0420 (male, Caucasian, 42

years) and the lowest in individual H0238 (male, African American, 3 months) (Table 6). These differences were mainly due to a ±80-fold higher K_m for methylation by individual H0238.

3.4 Development of the (individual) human PBK models and evaluation of their performance

The kinetic constants obtained from *in vitro* incubations with pooled and individual human tissue fractions were combined into PBK models to predict the bioavailability of quercetin aglycone. The average predicted bioavailability of quercetin aglycone was 0.005% of the dose and ranged between 0.001 and 0.04% of the dose for the individual human models at an average dietary intake of 0.4 mg/kg bw quercetin. Quercetin was completely metabolized within 1.5 h for all individuals and ~96% of the dose was converted to monoglucuronides. Among the mono-conjugates, quercetin-3′-O-glucuronide was predicted to be formed to the highest extent accounting for 53 to 57% of the dose.

Further conjugation of different monoglucuronides to di- and tri-conjugates was simulated. Because *in vivo* also quercetin-3′-O-sulfate has been detected in the plasma, the formation of this metabolite was included in the comparison between the model predictions and *in vivo* data, but given the low overall percentage of its formation (i.e < 3% of the dose), this metabolite was not simulated to be subject to further conjugation. In general, the fitted models showed comparable plasma levels of metabolites to the levels reported in literatures (i.e. within 1 to 4-fold) (Figure 4). Only for quercetin-3′-O-sulfate predictions were 4 to 44-fold lower than the reported values in the three studies [9-11]. For further development of the model for prediction of di- and tri-conjugates, parameters obtained with the data from the study of Lee *et al.* [9] with positive detection mode were used since these provided the best fit, with a 4-fold deviation between predicted and observed values for quercetin-3′-O-sulfate (Figure 4A). The fitted parameters obtained are displayed in the Table 7.

With the adequate predictions of the plasma levels of the different metabolites obtained by the (individual) human PBK models, the performance of models was further assessed by

comparing the predicted excretion of quercetin metabolites via urine, bile and intestinal enterocyte efflux back to lumen to the reported levels *in vivo* [10, 23, 24]. Figure 5 shows that the models adequately predicted urinary profiles with 1 to 4-fold and 1 to 7-fold accuracy 4 h and 24 h after consumption of onions corresponding to dose levels of 0.46 mg/kg bw Q4´Gly and 0.49 mg/kg bw Q34´diGly [23] and 0.95 Q4´Gly and 0.96 mg/kg bw Q34´diGly [10]. After 72 h following consumption of 1.4 mg/kg bw ^{14}C-quercetin, 3.5 to 5.7% of the dose was recovered in the urine which is 1 to 2-fold lower than the model prediction of 7.5% of the dose at the same dose [24]. In the same study 52.1 ± 6.4% of the dose was recovered as $^{14}CO_2$ in the expired air. This value can be used to evaluate the biliary excretion and intestinal efflux back to lumen, because $^{14}CO_2$ is likely a product of microorganisms present in the intestinal lumen [27]. The predicted biliary excretion (74% of the dose) together with intestinal enterocyte efflux back to lumen (16% of the dose) is 2-fold higher than the reported CO_2 level *in vivo* at the same dose.

The key parameters that influence the predicted plasma $AUC_{0\text{-}24h}$ of all quercetin metabolites in human at a dose of 0.4 mg/kg bw quercetin were assessed and are shown in Figure 6. The plasma $AUC_{0\text{-}24h}$ of quercetin metabolites are mainly influenced by parameters determining concentration in liver, namely liver volume, biliary excretion rate constant and S9 protein content in liver. The blood/plasma ratio is also found to have a great influence on the prediction as it determines the concentration of metabolites in plasma. The kinetic parameters for formation of mono-conjugates especially in the liver as well as the correction factors for the V_{max} and the K_m for formation of di- and tri-conjugates, have an influence on the plasma $AUC_{0\text{-}24h}$ of quercetin metabolites. Other parameters including partition coefficients and blood flow rates to tissue do not have an effect on the predicted plasma $AUC_{0\text{-}24h}$ of quercetin metabolites.

3.5 Model simulations

Figure 7 shows the predicted regiospecificity of the six metabolites with the highest plasma $AUC_{0\text{–}24h}$ at a dose of 0.4 mg/kg bw quercetin (average dietary intake) and a dose of 12

mg/kg bw quercetin (average supplementary intake), including interindividual human variation and species differences. At a dose of 0.4 mg/kg bw, quercetin-3´-O-glucuronide was predicted to be the major metabolite for 19 out of 20 individual human subjects accounting for 19 to 42% of the total plasma $AUC_{0\text{-}24h}$ (Figure 7A). However, individual H0270 (male, Caucasian, 5 months) that expressed a high level of glucuronidation at the 3-OH, was predicted to have mainly quercetin-3,3´-O-diglucuronide in the plasma accounting for 43% of the total plasma $AUC_{0\text{-}24h}$. At a dose of 12 mg/kg bw quercetin, quercetin-3´-O-glucuronide becomes the major metabolite for all individuals (Figure 7B) due to saturation of other reactions at higher dose levels.

Comparison of the predicted levels of the major circulating metabolites of quercetin in humans to those previously predicted for male rats revealed major species differences in circulating metabolites [12]. In male rats a di- and tri-conjugate of quercetin containing a glucuronic acid, sulfate and/or methyl moiety were predicted to be the major circulating metabolites of quercetin at both average dietary and supplementary intake. The differences between male rats and human in regiospecificity of circulating metabolites were especially a result of the catalytic efficiency and regioselectivity, which the primary metabolites are formed (Table 7).

4. Discussion

Flavonoid aglycones have been intensively used *in vitro* to elucidate its mode of actions underlying the health beneficial effects of flavonoids. However, *in vivo* effects of flavonoids are ultimately dependent on the bioavailability of flavonoid aglycones and its metabolites. In the present study, (individual) human PBK models for quercetin were defined by integrating kinetic data obtained from *in vitro* incubations with (individual) human tissue fractions, providing information on the nature and time-dependent formation of quercetin and its metabolites in humans and interindividual human variation herein. The outcomes obtained allowed to tentatively predict the regiospecificity of the major circulating metabolites in human, which were compared to those previously predicted with a PBK model for quercetin in male rat to elucidate species differences [12]. The focus was on metabolites that formed by intestinal and liver tissue. Potential metabolic conversion by gut microbiota, was indirectly accounted for by simulating biliary excretion and intestinal enterocyte efflux back to lumen.

The bioavailability of quercetin aglycone in (individual) human subjects was predicted to be limited ranging from 0.001 to 0.04% of the dose at an average dietary intake of 0.4 mg/kg bw quercetin. This result is in agreement with results from previous studies of Gugler *et al.* [28] and Graefe *et al*. reporting that no quercetin aglycone can be detected in human plasma after consumption of 50 to 60 mg/kg bw quercetin or 2.2 mg/kg bw Q4´Gly [29]. The low bioavailability of quercetin aglycone is due to extensive first pass metabolism of quercetin in the body, especially via glucuronidation as ~96% of the dose was predicted in the present study to be converted to monoglucuronides within 1.5 h.

Quercetin-3´-O-glucuronide was predicted to be the major circulating metabolite of quercetin in most individual humans both at a dose relevant to average dietary and supplementary intake of 0.4 and 12 mg/kg bw, respectively. In one individual, however, a glucuronide at the 3 position of quercetin-3´-O-glucuronide was the major circulating metabolite, indicating a swift further conversion of quercetin-3´-O-glucuronide in this individual. The importance of quercetin-

3′-O-glucuronide and its further conjugates as major metabolites of quercetin is supported by a study of Mullen *et al*. in which quercetin-3′-O-glucuronide and di- and tri-conjugates containing a glucuronide moiety were the major metabolites in the urine after consumption of onions [10]. However, these metabolites were not observed to be the major metabolites in the plasma, which was observed to mainly contain quercetin-3′-O-sulfate [10]. A more recent study by Lee *et al.*, , revealed that quercetin conjugates containing glucuronide moiety are the most important metabolites present in human plasma, when quantified with LC-MS in positive ion mode [9]. In the study of Lee et al. the regiospecificity of these metabolites was not determined, and the importance of especially quercetin-3′-O-glucuronide as a major circulating can therefore not be confirmed based on this study.

Interindividual human variation was observed in the kinetic constants for glucuronidation, sulfation and methylation as determined with the incubations performed with the 20 individual human liver fractions of the present study (Table 4-6). These differences lead to a variation in the plasma concentrations of quercetin metabolites including a 4-fold variation in the predicted level of the major circulating metabolite, quercetin-3′-O-glucuronide. This variation was mainly a result of differences in glucuronidation efficiency at positions besides the 3′ position, rather than interindividual human variation for further conjugation of this metabolite to sulfate or methyl conjugates or formation of 3′-O-glucuronide itself. For example, the lowest plasma concentration of quercetin-3′-O-glucuronide was observed for individual H0270, who displayed the highest catalytic efficiency for further conjugation of quercetin-3′-O-glucuronide at the 3 position, resulting in quercetin-3,3′-O-diglucuronide as the major circulating metabolite for this individual. These results may suggest that especially and genetic- and lifestyle factors influencing the expression and/or activity of UGT enzymes involved in quercetin glucuronidation, including UGT1A1, UGT1A3, UGT1A8, UGT1A9, and UGT2B7 may influence the regiospecificity of circulating metabolites [16].

With the developed PBK models for quercetin in (individual) human subjects and the previously defined model for rats, also species differences in metabolism of quercetin could be evaluated. Whereas the major predicted circulating metabolites of quercetin in humans are monoglucuronides and predominantly quercetin-3´-O-glucuronide, the major circulating metabolites in rats were di- and tri-conjugates containing glucuronic acid, sulfate and/or methyl moiety (Figure 7). These differences are partly due to a 2.3–fold higher metabolic conversion in rats as compared with humans, resulting in a faster further conversion of the monoglucuronides. A higher rate of glucuronidation in rats compared with human is more commonly observed. For example, Furukawa *et al.*, reported that glucuronidation of quercetin in rat is 2.2-fold more efficient than in human based on the catalytic efficiencies obtained from *in vitro* incubations with rat and human intestinal microsomes [30]. Glucuronidation of related flavonoids, including hesperetin, kaempferol, genistein, daidzein, and glycitein has been reported to be more efficient in rat than in human as observed in *in vitro* incubations with tissue fractions [31-34]. Studies on the glucuronidation of other compounds including buprenorphine, entacapone, ezetimibe, mycophenolic acid, and tolcapone further support that rat has higher glucuronidating activities than human based on the catalytic efficiencies obtained from *in vitro* incubations with rat and human intestinal microsomes [30]. Also species differences in the tentatively identified regiospecificity of circulating metabolites were observed, as rats mainly show primary glucuronidation at the 4´-OH and humans at the 3´-OH and di- and tri-conjugates building further on these different mono-conjugates in both species. This differences in conversion of flavonoids may be a result of differences in the size and shape of the binding pocket of different enzymes involved in the reactions [35]. Glucuronidation of quercetin in humans has been identified to be catalyzed by UGT1A1, UGT1A8 and UGT1A9 based on incubations with recombinant enzymes [16], whereas glucuronidation in rats has been linked to UGT1A1 and UGT1A7 activity in an *in vitro* study with rat tissue fractiosn [36]. Especially UGT1A1 has been reported to preferentially convert flavones at the 3´-OH (the primary glucuronide formed in humans in the present study)

[35]. A difference in contribution of this enzyme to the total glucuronidation activity between the two species might therefore explain the observed differences in primary metabolites that are formed and consequently the secondary and tertiary metabolites that build upon these primary glucuronides.

Considering that the nature and the position of flavonoid conjugation could be a key factor determining biological activity of flavonoids *in vivo* [37], the observed differences between individual human subjects in circulating metabolites could indicate critical differences in sensitivity to health beneficial effects. In addition, the differences between rats and humans may suggest that the biological effects of flavonoids observed in rats may not necessary be relevant for the human situation. At present little is known about the biological activity of flavonoid metabolites. Metabolism does not always result in a reduced biological activity of flavonoids [37]. In addition, biological activity might be a result of the extent by which the flavonoids are deconjugated to the active aglycone in a tissue [38, 39]. The results obtained with the PBK model allow to identify which metabolites will be relevant to study for their biological activity or to use in incubations to determine deconjugation, which are for humans predominantly quercetin-3´-O-glucuronide and conjugates of this metabolite.

Overall, the newly developed PBK model adequately predicted overall plasma concentrations of quercetin and its metabolites including mono-, di-, and tri-conjugates and provides an indication of the nature of the circulating metabolites of quercetin in plasma of humans and interindivdiual human variation herein. Significant species differences occur in the major circulating metabolites of quercetin in the systemic circulation indicating that rat is not an adequate model to study effects of quercetin in man. The developed PBK models can also be used to guide experimental design of *in vitro* experiments with flavonoids, especially to take into account the relevance of metabolism and the contribution of metabolites to the biological activity of flavonoids in humans.

Acknowledgements

This research was financially supported by the Ministry of Science and Technology of Thailand through a Royal Thai Government Scholarship awarded to Rungnapa Boonpawa for conducting her PhD thesis in The Netherlands.

Conflict of interest

The authors state no conflict of interest.

5. References

[1] Neuhouser ML. Review: Dietary flavonoids and cancer risk: Evidence from human population studies. Nutr Cancer. 2004;50:1-7.

[2] Perez-Vizcaino F, Duarte J. Flavonols and cardiovascular disease. Mol Aspects Med. 2010;31:478-94.

[3] Larson A, Symons JD, Jalili T. Quercetin: A treatment for hypertension?—A review of efficacy and mechanisms. Pharmaceuticals. 2010;3:237-50.

[4] Aguirre L, Noemi Arias M, Macarulla T, Gracia A, Portillo MP. Beneficial effects of quercetin on obesity and diabetes. Open Nutraceuticals J. 2011;4:189-98.

[5] de Boer VCJ, Dihal AA, van der Woude H, Arts ICW, Wolffram S, Alink GM, et al. Tissue distribution of quercetin in rats and pigs. J Nutr. 2005;135:1718-25.

[6] Németh K, Plumb GW, Berrin J-G, Juge N, Jacob R, Naim HY, et al. Deglycosylation by small intestinal epithelial cell β-glucosidases is a critical step in the absorption and metabolism of dietary flavonoid glycosides in humans. Eur J Nutr. 2003;42:29-42.

[7] Day AJ, Gee JM, DuPont MS, Johnson IT, Williamson G. Absorption of quercetin-3-glucoside and quercetin-4′-glucoside in the rat small intestine: the role of lactase phlorizin hydrolase and the sodium-dependent glucose transporter. Biochemical Pharmacology. 2003;65:1199-206.

[8] Graf BA, Mullen W, Caldwell ST, Hartley RC, Duthie GG, Lean MEJ, et al. Disposition and metabolism of [2-^{14}C] quercetin-4'-glucoside in rats. Drug Metabolism and Disposition. 2005;33:1036-43.

[9] Lee J, Ebeler SE, Zweigenbaum JA, Mitchell AE. UHPLC-(ESI)QTOF MS/MS profiling of quercetin metabolites in human plasma postconsumption of applesauce enriched with apple peel and onion. Journal of Agricultural and Food Chemistry. 2012;60:8510-20.

[10] Mullen W, Edwards CA, Crozier A. Absorption, excretion and metabolite profiling of methyl-, glucuronyl-, glucosyl- and sulpho-conjugates of quercetin in human plasma and urine after ingestion of onions. Br J Nutr. 2006;96:107-16.

[11] Day AJ, Mellon F, Barron D, Sarrazin G, Morgan MRA, Williamson G. Human metabolism of dietary flavonoids: Identification of plasma metabolites of quercetin. Free Radic Res. 2001;35:941-52.

[12] Boonpawa R, Spenkelink A, Rietjens IMCM, Punt A. A physiologically based kinetic (PBK) model describing plasma concentrations of quercetin and its metabolites in rats. Biochemical Pharmacology. 2014;89:287-99.

[13] Fisher MB, Campanale K, Ackermann BL, VandenBranden M, Wrighton SA. In vitro glucuronidation using human liver microsomes and the pore-forming peptide alamethicin. Drug Metabolism and Disposition. 2000;28:560-6.

[14] Diez-Roux G, Ballabio A. Sulfatases and human disease. Annual Review of Genomics and Human Genetics. 2005;6:355-79.

[15] Parenti G, Meroni G, Ballabio A. The sulfatase gene family. Current Opinion in Genetics & Development. 1997;7:386-91.

[16] Boersma MG, van der Woude H, Bogaards J, Boeren S, Vervoort J, Cnubben NHP, et al. Regioselectivity of phase II metabolism of luteolin and quercetin by UDP-glucuronosyl transferases. Chem Res Toxicol. 2002;15:662-70.

[17] van der Woude H, Boersma MG, Vervoort J, Rietjens IMCM. Identification of 14 quercetin phase II mono- and mixed conjugates and their formation by rat and human phase II in vitro model systems. Chem Res Toxicol. 2004;17:1520-30.

[18] Walle T, Otake Y, Walle UK, Wilson FA. Quercetin glucosides are completely hydrolyzed in ileostomy patients before absorption. J Nutr. 2000;130:2658-61.

[19] Petri N, Tannergren C, Holst B, Mellon FA, Bao Y, Plumb GW, et al. Absorption/metabolism of sulforaphane and quercetin, and regulation of phase II enzymes, in human jejunum in vivo. Drug Metabolism and Disposition. 2003;31:805-13.

[20] Chen X, Yin OQP, Zuo Z, Chow MSS. Pharmacokinetics and modeling of quercetin and metabolites. Pharm Res. 2005;22:892-901.

[21] Brown RP, Delp MD, Lindstedt SL, Rhomberg LR, Beliles RP. Physiological parameter values for physiologically based pharmacokinetic models. Toxicol Ind Health. 1997;13:407-84.

[22] DeJongh J, Verhaar HJM, Hermens JLM. A quantitative property-property relationship (QPPR) approach to estimate in vitro tissue-blood partition coefficients of organic chemicals in rats and humans. Arch Toxicol. 1997;72:17-25.

[23] Hong Y-J, Mitchell AE. Metabolic profiling of flavonol metabolites in human urine by liquid chromatography and tandem mass spectrometry. Journal of Agricultural and Food Chemistry. 2004;52:6794-801.

[24] Walle T, Walle UK, Halushka PV. Carbon dioxide is the major metabolite of quercetin in humans. J Nutr. 2001;131:2648-52.

[25] Simcyp. Simcyp prediction tools-fu. [Website]. Available from: https://members.simcyp.com/account/tools/fu/ [Accessed on: 07-07-2014]. 2014.

[26] Simcyp. Simcyp prediction tools - blood to plasma partition ratio (B/P).[Website]. Available from: https://members.simcyp.com/account/tools/BP/ [Accessed on: 7-7-2014]. 2014.

[27] Ueno I, Nakano N, Hirono I. Metabolic fate of [^{14}C] quercetin in the ACl rat. Jpn J Exp Med. 1983;53:41-50.

[28] Gugler R, Leschik M, Dengler HJ. Disposition of quercetin in man after single oral and intravenous doses. 1975;9:229-34.

[29] Graefe EU, Wittig J, Mueller S, Riethling A-K, Uehleke B, Drewelow B, et al. Pharmacokinetics and bioavailability of quercetin glycosides in humans. J Clin Pharmacol. 2001;41:492-9.

[30] Furukawa T, Naritomi Y, Tetsuka K, Nakamori F, Moriguchi H, Yamano K, et al. Species differences in intestinal glucuronidation activities between humans, rats, dogs and monkeys. Xenobiotica. 2014;44:205-16.

[31] Brand W, Boersma MG, Bik H, Hoek-van den Hil EF, Vervoort J, Barron D, et al. Phase II metabolism of hesperetin by individual UDP-glucuronosyltransferases and sulfotransferases and rat and human tissue samples. Drug Metabolism and Disposition. 2010;38:617-25.

[32] Otake Y, Hsieh F, Walle T. Glucuronidation versus oxidation of the flavonoid galangin by human liver microsomes and hepatocytes. Drug Metabolism and Disposition. 2002;30:576-81.

[33] Barve A, Chen C, Hebbar V, Desiderio J, Saw CL-L, Kong A-N. Metabolism, oral bioavailability and pharmacokinetics of chemopreventive kaempferol in rats. Biopharmaceutics & drug disposition. 2009;30:356-65.

[34] Islam MA, Punt A, Spenkelink B, Murk AJ, Rolaf van Leeuwen FX, Rietjens IMCM. Conversion of major soy isoflavone glucosides and aglycones in in vitro intestinal models. Mol Nutr Food Res. 2014;58:503-15.

[35] Wu B, Basu S, Meng S, Wang X, Zhang S, Hu M. Regioselective sulfation and glucuronidation of phenolics: insights into the structural basis of conjugation. Current drug metabolism. 2011;12:900-16.

[36] Bolling BW, Court MH, Blumberg JB, Chen C-Y. Microsomal quercetin glucuronidation in rat small intestine depends on age and segment. Drug Metabolism and Disposition. 2011.

[37] Beekmann K, Actis-Goretta L, van Bladeren PJ, Dionisi F, Destaillats F, Rietjens IMCM. A state-of-the-art overview of the effect of metabolic conjugation on the biological activity of flavonoids. Food Funct. 2012;3:1008-18.

[38] Galindo P, Rodriguez-Gómez I, González-Manzano S, Dueñas M, Jiménez R, Menéndez C, et al. Glucuronidated quercetin lowers blood pressure in spontaneously hypertensive rats via deconjugation. PLoS One. 2012;7:e32673.

[39] Bartholomé R, Haenen G, Hollman PCH, Bast A, Dagnelie PC, Roos D, et al. Deconjugation kinetics of glucuronidated phase II flavonoid metabolites by β-glucuronidase from neutrophils. Drug Metab Pharmacokinet. 2010;25:379-87.

Figure captions

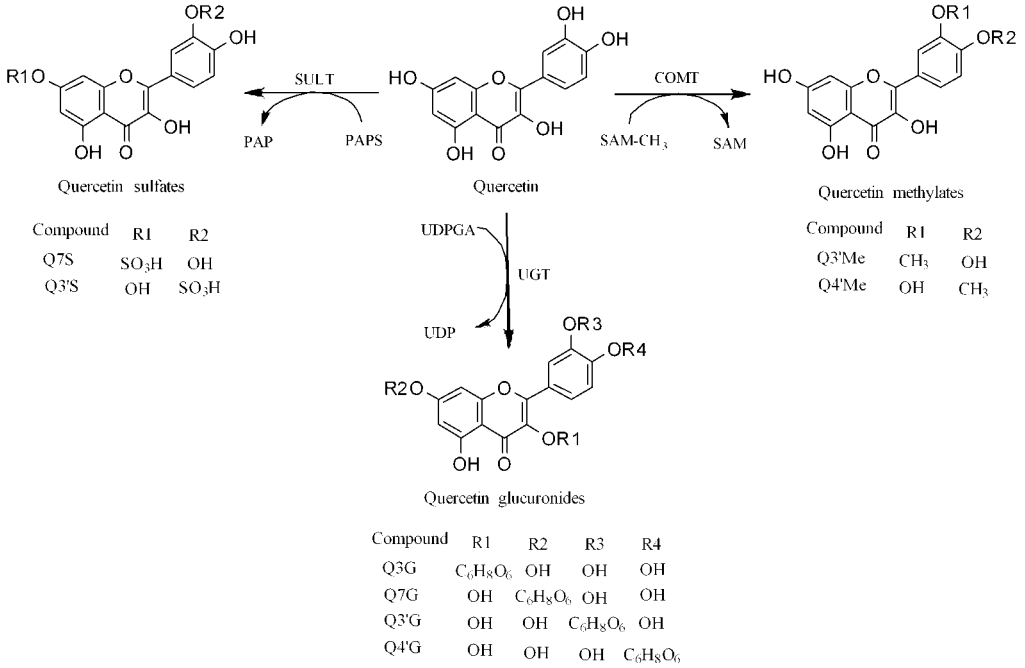

Figure 1. Conversion of quercetin to different possible mono-conjugates [12].

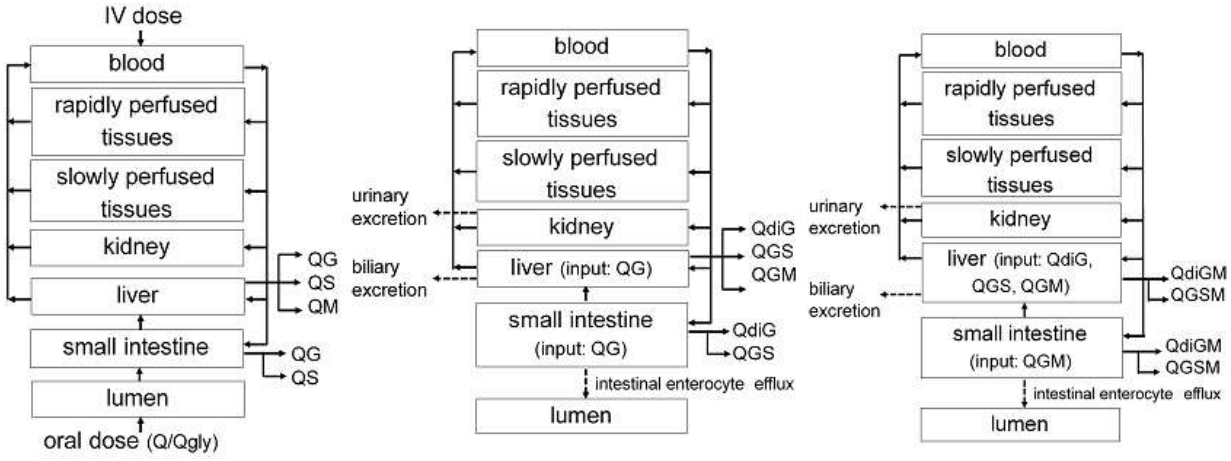

Figure 2. Schematic diagram of the PBK models for prediction of the formation of mono-conjugates (A), di-conjugates (B), and tri-conjugates (C).

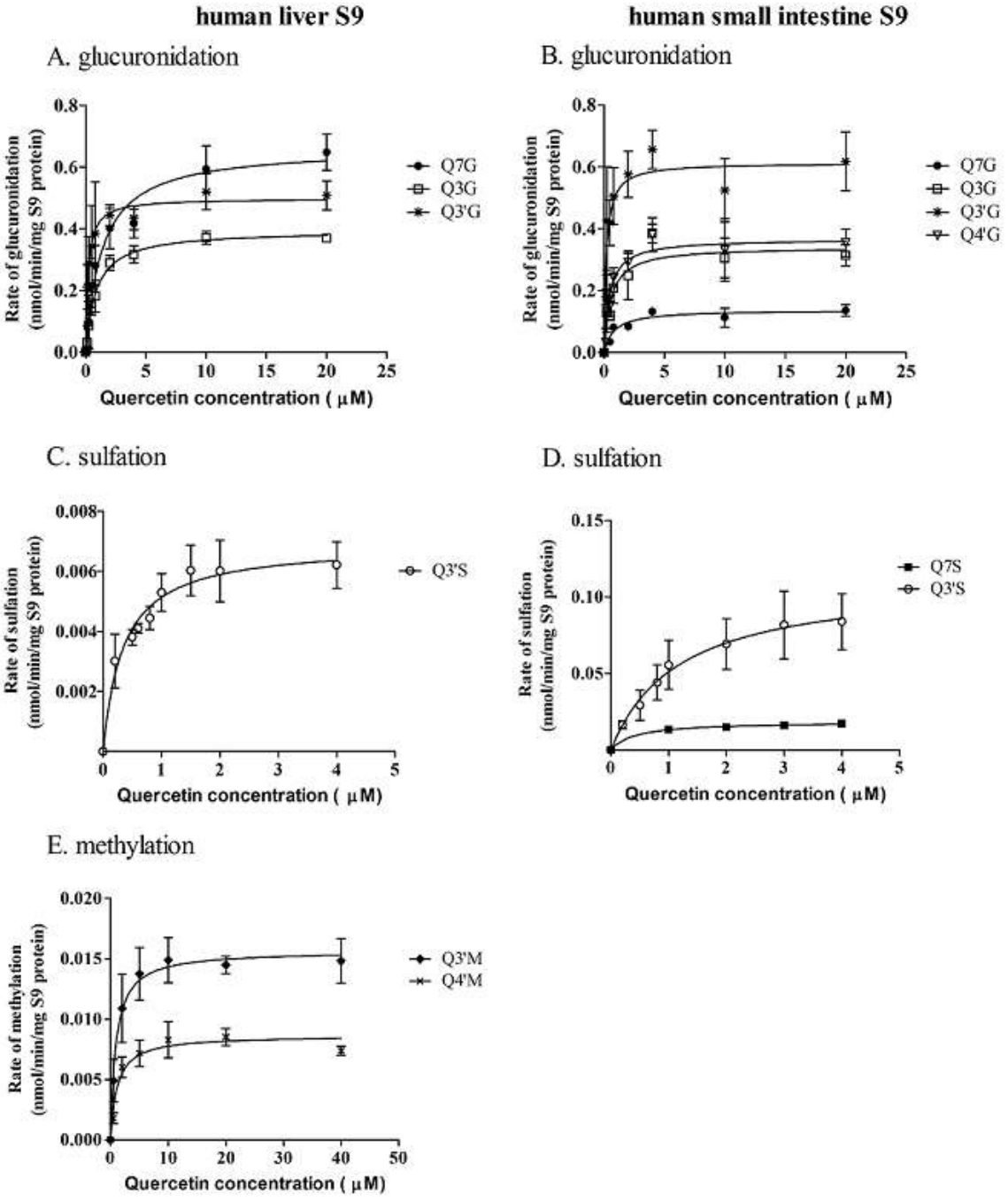

Figure 3. Quercetin concentration-dependent formation of mono-conjugates by pooled mixed-gender human liver S9 (A, C, and E) or small intestine S9 (B and D); quercetin (Q), glucuronide (G), sulfate (S) and methyl conjugate (M).

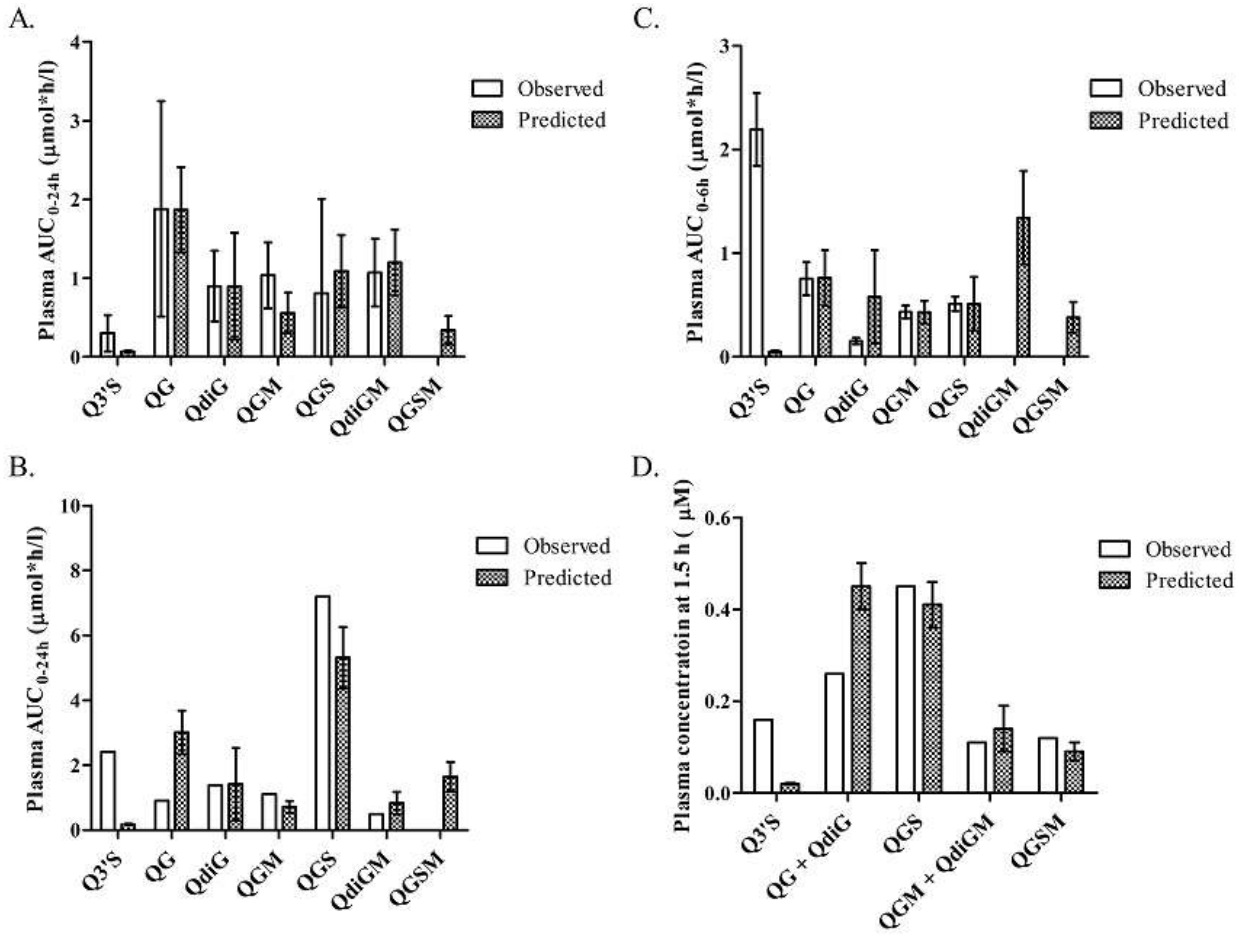

Figure 4. Prediction on plasma profiles of quercetin metabolites in (individual) human subjects compared to the reported levels *in vivo* at a dose of 0.64 mg/kg bw Q4′Gly and 0.70 mg/kg bw Q34′diGly as detected with positive (A) and negative detection mode (B) [9], at a dose of 0.95 mg/kg bw Q4′Gly and 0.96 mg/kg bw Q34′diGly (C) [10], at a dose of 0.56 mg/kg bw Q4′Gly and 0.53 mg/kg bw Q34′diGly [11] (D); quercetin (Q), glucuronide (G), sulfate (S) and methyl conjugate (M).

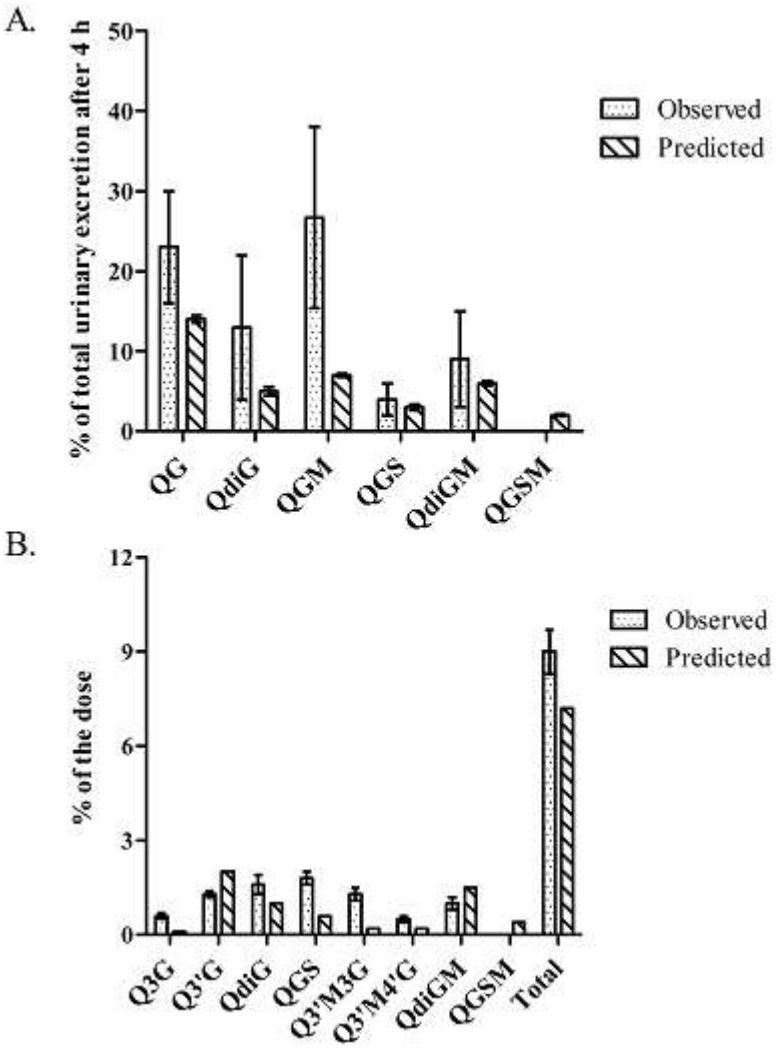

Figure 5. Prediction on urinary profiles of quercetin metabolites as compared with the reported levels *in vivo* at a dose of 0.46 mg/kg bw Q4′Gly and 0.49 mg/kg bw Q34′diGly (A) [23] and 0.95 mg/kg bw Q4′Gly and 0.96 mg/kg bw Q34′diGly (B) [10]; quercetin (Q), glucuronide (G), sulfate (S) and methyl conjugate (M).

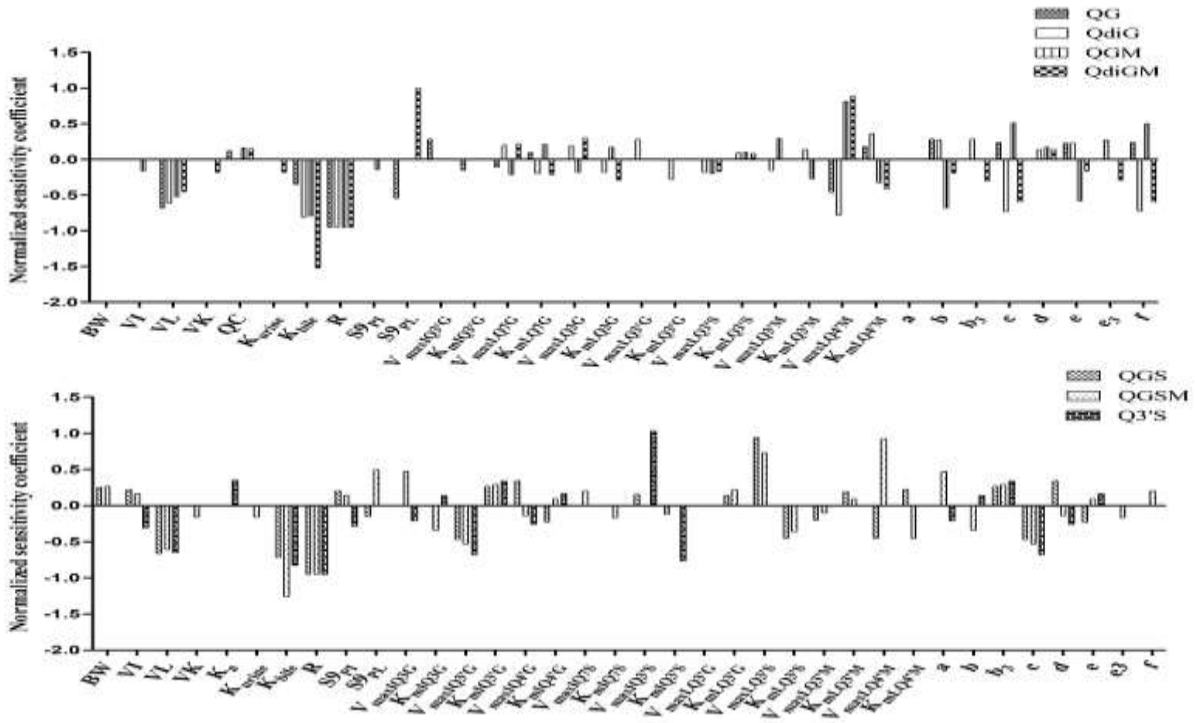

Figure 6. Sensitivity analysis of the predicted plasma AUC0-24h of quercetin monoglucuronides (QG), quercetin diglucuronides (QdiG), quercetin glucuronide methyl conjugates (QGM), quercetin glucuronide sulfate conjugates (QGS), quercetin diglucuronide methyl conjugates (QdiGM), quercetin glucuronide sulfate methyl conjugates (QGSM), and quercetin-3′-O-sulfate (Q3′S) in human exposed to 0.4 mg (kg bw) -1 quercetin. The parameters are stand for: BW = body weight, VTi = tissue volume (Ti = I (small intestine), L (liver), K (kidney)), QC = cardiac output, K_a = uptake rate of quercetin, K_{urine} = urinary excretion rate constant, K_{bile} = biliary excretion rate constant, R = blood/plasma ratio, S9PI = small intestinal S9 protein content, S9PL = liver S9 protein content, V_{max} and K_m = the maximum rate of formation and the Michaelis-Menten constant for formation of metabolite (G (glucuronide), S (sulfate), M (methylate), and correction factors for the reduction of V_{max} for sulfate-conjugates of QG or QGM (a), methylate-conjugates of QG or QGS (b), methylate-conjugated of QdiG (b_3), glucuronide-conjugates of QG or QGM (c) and for the induction of K_m for sulfate-conjugates of QG or QGM (d), methylate-conjugates of QG or QGS (e), methylate-conjugated of QdiG (e_3), glucuronide-conjugates of QG or QGM (f).

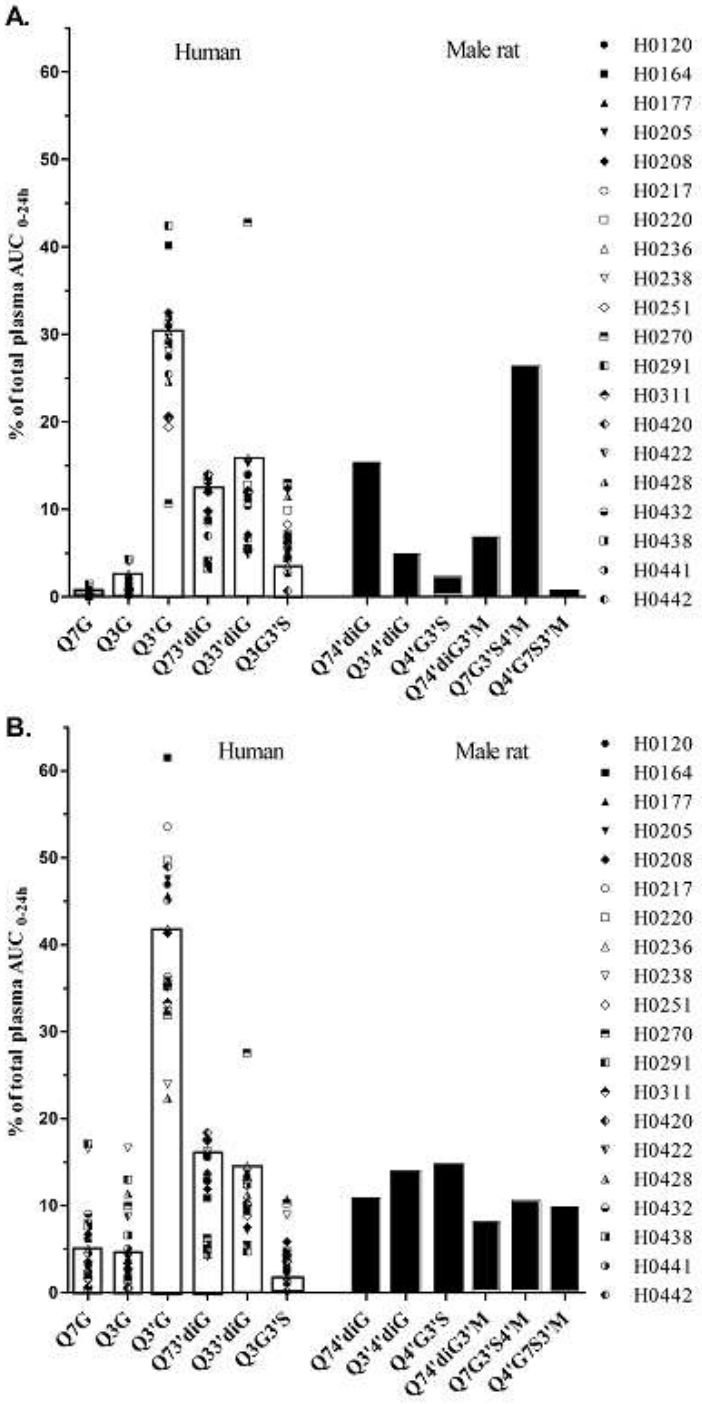

Figure 7. Prediction on regiospecificity of the major circulating metabolites of quercetin in (individual) human subjects as compared with male rat [12] at a dose of 0.4 (A) and 12 mg/kg bw quercetin (B); quercetin (Q), glucuronide (G), sulfate (S) and methyl conjugate (M). Data were expressed as % of total plasma $AUC_{0\text{-}24h}$. The bar and dots present the prediction obtained from the average and individual models.

Tables

Table 1. Physiological parameters used in the PBK model for quercetin in human and male rat [21]

Parameters	Symbol	Human	Male rat
Body weight (kg)	BW	70	0.25
Tissue volumes (% body weight)			
lumen	VLu	1.4	5
small intestine	VI	0.9	1.4
liver	VL	2.6	3.4
kidney	VK	0.4	0.7
rapidly perfused tissues	VR	4	3.2
slowly perfused tissues	VS	75.7	74.6
blood	VB	7.9	7.4
Cardiac output (l/h)	QC	310.4	5.4
Blood flow to tissue (% cardiac output)			
small intestine	QI	18.1	15.1
liver (exclude portal vein)	QL	4.6	9.9
kidney	QK	17.5	14.1
rapidly perfused tissues	QR	29.8	36.9
slowly perfused tissues	QS	30	24

Table 2. Physio-chemical parameters of quercetin and its metabolites in humans

Compound	Log*P*[1]	*p*Ka[2]	fu[3]	R[4]	Tissue:blood partition coefficients[5]				
					Small intestine	Liver	Kidney	Rapidly perfused tissue	Slowly perfused tissue
quercetin	1.99	6.31	0.071	0.69	2.46	2.46	1.42	1.83	1.81
quercetin-7-O-glucuronide	-0.47	2.73	0.362	0.61	0.62	0.62	0.79	0.72	0.76
quercetin-3-O-glucuronide	0.62	2.76	0.186	0.64	0.77	0.77	0.88	0.91	0.85
quercetin_3'-O-glucuronide	0.00	2.78	0.619	0.62	0.65	0.65	0.81	0.78	0.78
quercetin-4'-O-glucuronide	-0.12	2.78	0.615	0.62	0.64	0.64	0.80	0.76	0.77
quercetin-7-O-sulfate	1.20	-4.92	0.123	0.66	1.11	1.11	1.01	1.16	1.04
quercetin-3'-O-sulfate	1.18	-4.37	0.125	0.66	1.09	1.09	1.00	1.14	1.03
3'-O-methylquercetin	2.79	6.31	0.038	0.72	5.27	5.27	2.39	3.30	3.41
4'-O-methylquercetin	2.67	6.31	0.041	0.72	4.82	4.82	2.20	3.02	3.15
quercetin diglucuronides	-2.74				0.59	0.59	0.76	0.65	0.75
quercetin glucuronide sulfate conjugates	-2.20				0.59	0.59	0.76	0.65	0.75
quercetin glucuronide methyl conjugates	-0.16				0.64	0.64	0.80	0.76	0.77
quercetin diglucuronide methyl conjugates	-2.29				0.59	0.59	0.76	0.65	0.75
quercetin glucuronide sulfate methyl conjugates	-1.81				0.59	0.59	0.76	0.66	0.75

[1] Log*P* values for quercetin and its mono-conjugates were obtained from Scifinder (American Chemical Society, USA), while CLog*P* values for di- and tri-conjugates were calculated using ChemBio3D Ultra 2010 (Cambridgesoft, USA).
[2] *p*Ka values were obtained from Scifinder (American Chemical Society, USA).
[3] Fraction unbound (fu) was calculated using Simcyp prediction tools – fu [25].
[4] Blood/plasma ratio (R) was calculated using Simcyp prediction tools - blood to plasma partition ratio [26].
[5]Tissue:blood partition coefficients were calculated based on method described by DeJongh *et al.* [22].

Table 3. Kinetic constants for mono-conjugates of quercetin with pooled mixed-gender human tissues S9 fractions

Metabolite	**Organ**	$K_{m(app)}$ (μM)	$V_{max(app)}$ (nmol/min /mg S9)	***In vitro* catalytic efficiency** (min /mg S9)[1]
quercetin-7-O-glucuronide	small intestine	0.84 ± 0.23	0.14 ± 0.01	0.17
quercetin-3-O-glucuronide	small intestine	0.56 ± 0.15	0.34 ± 0.02	0.61
quercetin-3'-O-glucuronide	small intestine	0.20 ± 0.05	0.61 ± 0.03	3.05
quercetin-4'-O-glucuronide	small intestine	0.46 ± 0.12	0.37 ± 0.02	0.80
quercetin-7-O-sulfate	small intestine	0.41 ± 0.14	0.02 ± 0.001	0.05
quercetin-3'-O-sulfate	small intestine	1.17 ± 0.35	0.11 ± 0.01	0.09
quercetin-7-O-glucuronide	liver	1.37 ± 0.04	0.66 ± 0.04	0.48
quercetin-3-O-glucuronide	liver	0.87 ± 0.14	0.39 ± 0.02	0.45
quercetin-3'-O-glucuronide	liver	0.21 ± 0.08	0.40 ± 0.02	2.67
quercetin-4'-O-glucuronide	liver	nd	nd	nd
quercetin-7-O-sulfate	liver	nd	nd	nd
quercetin-3'-O-sulfate	liver	0.35±0.07	0.01±0.0004	0.03
3'-O-methylquercetin	liver	0.93 ± 0.21	0.02 ± 0.001	0.02
4'-O-methylquercetin	liver	1.14 ± 0.27	0.01 ± 0.0004	0.01

[1] $V_{max(app)}/ K_{m(app)}$

Table 4. Kinetic constants for formation of quercetin monoglucuronides obtained from *in vitro* incubations with 20 individual human liver S9 fractions

Individual liver S9	Description (sex, age, race)	Quercetin-7-O-glucuronide			Quercetin-3-O-glucuronide			Quercetin-3'-O-glucuronide		
		$K_{m(app)}$ (µM)	$V_{max(app)}$ (nmol min/mg S9)	*In vitro* catalytic efficiency[1]	$K_{m(app)}$ (µM)	$V_{max(app)}$ (nmol min/mg S9)	*In vitro* catalytic efficiency[1]	$K_{m(app)}$ (µM)	$V_{max(app)}$ (nmol min/mg S9)	*In vitro* catalytic efficiency[1]
H0120	female, 57, Caucasian	0.49 ± 0.17	0.42 ± 0.03	0.86	0.49 ± 0.17	0.33 ± 0.02	0.67	0.05 ± 0.04	0.47 ± 0.03	9
H0164	male, 30, Caucasian	0.98 ± 0.20	0.33 ± 0.02	0.34	0.98 ± 0.20	0.25 ± 0.01	0.26	0.06 ± 0.02	0.47 ± 0.02	8
H0177	female, 45, Caucasian	1.42 ± 0.35	0.75 ± 0.05	0.53	0.38 ± 0.10	0.17 ± 0.01	0.45	0.08 ± 0.02	0.38 ± 0.01	5
H0205	female, 48, Caucasian	0.96 ± 0.24	0.71 ± 0.05	0.74	0.62 ± 0.17	0.37 ± 0.03	0.60	0.14 ± 0.07	0.83 ± 0.09	6
H0208	female, 78, Caucasian	0.76 ± 0.13	0.46 ± 0.02	0.61	0.56 ± 0.07	0.21 ± 0.01	0.38	0.12 ± 0.04	0.37 ± 0.02	3
H0217	female, 66, Caucasian	0.94 ± 0.27	0.59 ± 0.05	0.63	0.75 ± 0.17	0.33 ± 0.02	0.44	0.03 ± 0.03	0.47 ± 0.03	16
H0220	female, 33, Caucasian	0.64 ± 0.12	0.51 ± 0.02	0.80	0.60 ± 0.10	0.34 ± 0.01	0.57	0.06 ± 0.03	0.56 ± 0.04	9
H0236	male, 17, Asian	1.08 ± 0.22	0.75 ± 0.04	0.69	0.67 ± 0.15	0.44 ± 0.03	0.66	0.23 ± 0.05	0.62 ± 0.03	3
H0238	male, 3 m, African American	1.02 ± 0.13	0.23 ± 0.01	0.23	0.13 ± 0.08	0.12 ± 0.01	0.92	0.66 ± 0.08	0.17 ± 0.01	0.3
H0251	female, 42, Caucasian	0.82 ± 0.15	1.18 ± 0.06	1.44	1.03 ± 0.16	0.73 ± 0.03	0.71	0.14 ± 0.06	1.16 ± 0.09	8
H0270	male, 5 m, Caucasian	0.76 ± 0.16	0.38 ± 0.02	0.50	0.02 ± 0.02	0.21 ± 0.01	10.50	0.07 ± 0.05	0.65 ± 0.06	9
H0291	female, 18, Caucasian	1.81 ± 0.31	0.30 ± 0.01	0.17	0.87 ± 0.12	0.16 ± 0.01	0.18	0.72 ± 0.15	0.24 ± 0.01	0.3
H0311	male, 21, Hispanic	0.66 ± 0.11	0.88 ± 0.04	1.33	0.35 ± 0.08	0.40 ± 0.02	1.14	0.12 ± 0.06	0.73 ± 0.06	6
H0420	male, 42, Caucasian	0.36 ± 0.08	0.57 ± 0.03	1.60	0.53 ± 0.14	0.35 ± 0.02	0.66	0.06 ± 0.04	1.40 ± 0.13	23
H0422	male, 69, Caucasian	1.77 ± 0.29	0.48 ± 0.02	0.27	0.95 ± 0.15	0.32 ± 0.01	0.34	0.37 ± 0.11	0.32 ± 0.02	1
H0428	female, 57, Caucasian	3.19 ± 0.82	1.13 ± 0.09	0.04	0.87 ± 0.19	0.91 ± 0.05	0.40	0.35 ± 0.16	0.44 ± 0.05	1
H0432	male, 60, African American	0.70 ± 0.52	0.60 ± 0.12	0.86	0.86 ± 0.63	0.40 ± 0.08	0.47	0.11 ± 0.13	0.38 ± 0.07	3
H0438	male, 56, Caucasian	2.33 ± 0.40	0.63 ± 0.03	0.27	0.36 ± 0.07	0.15 ± 0.01	0.42	0.19 ± 0.04	0.27 ± 0.01	1
H0441	male, 63, Caucasian	1.76 ± 0.23	0.83 ± 0.03	0.47	0.37 ± 0.08	0.23 ± 0.01	0.62	0.12 ± 0.05	0.48 ± 0.03	4
H0442	male, 49, Caucasian	2.38 ± 1.11	1.23 ± 0.17	0.52	0.35 ± 0.18	0.28 ± 0.04	0.80	0.18 ± 0.12	0.35 ± 0.05	2

[1] $V_{max(app)}$/ $K_{m(app)}$, ml/min/mg S9

Table 5. Kinetic constants for formation of quercetin monosulfates obtained from *in vitro* incubations with 20 individual human liver S9 fractions

Individual liver S9	Description (sex, age, race)	Quercetin-3'-O-sulfate		
		$K_{m(app)}$ (μM)	$V_{max(app)}$ (nmol min/mg S9)	*In vitro* catalytic efficiency[1]
H0120	female, 57, Caucasian	0.13 ± 0.06	0.010 ± 0.001	0.08
H0164	male, 30, Caucasian	0.11 ± 0.04	0.011 ± 0.001	0.10
H0177	female, 45, Caucasian	0.13 ± 0.06	0.003 ± 0.0003	0.02
H0205	female, 48, Caucasian	0.22 ± 0.03	0.010 ± 0.0003	0.05
H0208	female, 78, Caucasian	0.02 ± 0.02	0.015 ± 0.001	0.75
H0217	female, 66, Caucasian	0.11 ± 0.03	0.008 ± 0.0003	0.07
H0220	female, 33, Caucasian	0.04 ± 0.01	0.013 ± 0.0004	0.33
H0236	male, 17, Asian	0.02 ± 0.01	0.005 ± 0.0001	0.25
H0238	male, 3 m, African American	0.15 ± 0.07	0.010 ± 0.001	0.07
H0251	female, 42, Caucasian	0.01 ± 0.02	0.025 ± 0.002	2.50
H0270	male, 5 m, Caucasian	0.04 ± 0.03	0.019 ± 0.002	0.48
H0291	female, 18, Caucasian	0.57 ± 0.24	0.009 ± 0.001	0.02
H0311	male, 21, Hispanic	0.09 ± 0.03	0.016 ± 0.001	0.18
H0420	male, 42, Caucasian	0.76 ± 0.16	0.002 ± 0.0002	0.003
H0422	male, 69, Caucasian	0.06 ± 0.01	0.010 ± 0.0002	0.17
H0428	female, 57, Caucasian	0.02 ± 0.02	0.021 ± 0.001	1.19
H0432	male, 60, African American	0.12 ± 0.06	0.007 ± 0.001	0.06
H0438	male, 56, Caucasian	0.06 ± 0.04	0.012 ± 0.001	0.20
H0441	male, 63, Caucasian	0.09 ± 0.05	0.005 ± 0.0005	0.06
H0442	male, 49, Caucasian	0.03 ± 0.01	0.014 ± 0.001	0.47

[1] $V_{max(app)}$/ $K_{m(app)}$, ml/min/mg S9

Table 6. Kinetic constants for formation of quercetin methyl conjugates obtained from *in vitro* incubations with 20 individual human liver S9 fractions

Individual liver S9	Description (sex, age, race)	3'-O-methylquercetin			4'-O-methylquercetin		
		$K_{m(app)}$ (μM)	$V_{max(app)}$ (nmol min/mg S9)	*In vitro* catalytic efficiency[1]	$K_{m(app)}$ (μM)	$V_{max(app)}$ (nmol min/mg S9)	*In vitro* catalytic efficiency[1]
H0120	female, 57, Caucasian	0.65 ± 0.29	0.003 ± 0.0003	0.005	0.34 ± 0.29	0.001 ± 0.0002	0.003
H0164	male, 30, Caucasian	0.15 ± 0.13	0.001 ± 0.0001	0.01	4.46 ± 1.64	0.001 ± 0.0001	0.0002
H0177	female, 45, Caucasian	0.86 ± 0.19	0.010 ± 0.0005	0.01	1.07 ± 0.52	0.003 ± 0.0004	0.003
H0205	female, 48, Caucasian	0.40 ± 0.18	0.002 ± 0.0002	0.01	1.27 ± 0.85	0.001 ± 0.0002	0.001
H0208	female, 78, Caucasian	0.50 ± 0.30	0.002 ± 0.0003	0.004	2.63 ± 2.62	0.003 ± 0.001	0.001
H0217	female, 66, Caucasian	0.22 ± 0.23	0.005 ± 0.001	0.02	0.53 ± 0.24	0.003 ± 0.0002	0.01
H0220	female, 33, Caucasian	0.15 ± 0.12	0.002 ± 0.0002	0.01	9.01 ± 6.50	0.002 ± 0.001	0.0002
H0236	male, 17, Asian	0.47 ± 0.30	0.003 ± 0.0004	0.01	2.61 ± 2.37	0.002 ± 0.001	0.001
H0238	male, 3 m, African American	60.47 ± 61.52	0.010 ± 0.01	0.0002	37.11 ± 27.70	0.003 ± 0.001	0.0001
H0251	female, 42, Caucasian	0.57 ± 0.52	0.010 ± 0.002	0.02	0.78 ± 0.38	0.006 ±0.001	0.01
H0270	male, 5 m, Caucasian	0.14 ± 0.13	0.001 ± 0.0001	0.01	0.90 ± 0.60	0.0002 ± 0.0001	0.0002
H0291	female, 18, Caucasian	0.07 ± 0.08	0.002 ± 0.0002	0.03	2.05 ± 0.56	0.001 ± 0.0001	0.0005
H0311	male, 21, Hispanic	0.44 ± 0.08	0.010 ± 0.0003	0.02	1.00 ± 0.25	0.004 ± 0.0002	0.004
H0420	male, 42, Caucasian	0.46 ± 0.18	0.014 ± 0.001	0.03	1.29 ± 0.72	0.008 ± 0.001	0.01
H0422	male, 69, Caucasian	1.17 ± 0.48	0.020 ± 0.002	0.02	1.92 ± 1.00	0.010 ± 0.001	0.01
H0428	female, 57, Caucasian	2.44 ± 1.60	0.022 ± 0.004	0.01	4.63 ± 3.21	0.015 ± 0.004	0.003
H0432	male, 60, African American	1.49 ± 0.64	0.008 ± 0.001	0.01	3.22 ± 0.98	0.005 ± 0.0005	0.002
H0438	male, 56, Caucasian	0.50 ± 0.19	0.014 ± 0.001	0.03	1.39 ± 0.72	0.008 ± 0.001	0.006
H0441	male, 63, Caucasian	1.12 ± 0.86	0.007 ± 0.001	0.01	2.36 ± 2.06	0.003 ± 0.001	0.001
H0442	male, 49, Caucasian	0.56 ± 0.27	0.004 ± 0.0004	0.01	0.81 ± 0.53	0.002 ± 0.0003	0.002

[1] $V_{max(app)}$/ $K_{m(app)}$, ml/min/mg S9

Table 7. Kinetic parameters used in the PBK model for quercetin in human and male rat

Parameter	**Human**			**Male rat**[1]		
Uptake rate of quercetin (h-1) [20]	5.32			5.32		
Biliary excretion (h-1)	27			16		
Urinary excretion (h-1)	15			6.5		
Intestinal enterocyte efflux (l/h)	5			0.17		
Kinetics for mono-conjugates						
Small intestine	K_m[2]	V_{max}[3]	catalytic efficiency[4]	K_m[2]	V_{max}[3]	catalytic efficiency[4]
quercetin-7-O-glucuronide	0.84 ± 0.23	0.14 ± 0.01	0.11	0.28 ± 0.07	1.89 ± 0.1	4.62
quercetin-3-O-glucuronide	0.56 ± 0.15	0.34 ± 0.02	0.42	0.28 ± 0.07	0.47 ± 0.02	1.15
quercetin-3´-O-glucuronide	0.20 ± 0.05	0.61 ± 0.03	2.09	1.14 ± 0.24	0.92 ± 0.06	0.55
quercetin-4´-O-glucuronide	0.46 ± 0.12	0.37 ± 0.02	0.55	nd[5]	nd	
quercetin-7-O-sulfate	0.41 ± 0.14	0.02 ± 0.001	0.03	nd	nd	
quercetin-3´-O-sulfate	1.17 ± 0.35	0.11 ± 0.01	0.44	0.11 ± 0.03	0.01 ± 0.001	0.07
Liver						
quercetin-7-O-glucuronide	1.37 ± 0.04	0.66 ± 0.04	4.13	8.08 ± 2.6	6.11 ± 0.83	6.49
quercetin-3-O-glucuronide	0.87 ± 0.14	0.39 ± 0.02	3.85	nd	nd	
quercetin-3´-O-glucuronide	0.21 ± 0.08	0.40 ± 0.02	20	1.13 ± 0.29	1.46 ± 0.09	11
quercetin-4´-O-glucuronide	nd	nd		0.12 ± 0.04	0.66 ± 0.02	47
quercetin-7-O-sulfate	nd	nd	0.25	0.47 ± 0.2	0.04 ± 0.004	0.73
quercetin-3´-O-sulfate	0.35±0.07	0.01±0.0004	0.18	0.27 ± 0.07	0.14 ± 0.01	4.45
3´-O-methylquercetin	0.75±3.12	0.03±0.002	0.08	24 ± 3.39	0.46 ± 0.02	0.16
4´-O-methylquercetin	0.75±3.12	0.02±0.001	0.11	24 ± 3.39	0.23 ± 0.01	0.08
Correction factor for K_m						
sulfation of QG or QGM	5			2.2		
methylation of QG or QGS	1.6			1		
glucuronidation of QG or QGM	41			13		
methylation of QdiG	2			87		
Correction factor for V_{max}						
sulfation of QG or QGM		1.7			1.5	
methylation of QG or QGS		3			1	
glucuronidation of QG or QGM		20			12	
methylation of QdiG		2.9			31	

[1] Kinetic parameters for male rat were obtained from Boonpawa *et al*. [12]
[2] $K_{m(app)}$ expressed as µM.
[3] $V_{max(app)}$ expressed as nmol/min/mg S9 protein.
[4] catalytic efficiency (Scaled $V_{max}/K_{m(app)}$) expressed as l/h/g tissue; scaled V_{max} (µmol/h/g tissue) calculated from $V_{max(app)}$/(1000 nmol/µmol)*(60 min/h)*(mg S9/g tissue): 11.4 and 143 mg S9 yield in small intestine and in liver.
[5] nd = not detect able.